GSI

GSI-Preprint-98-21
April 1998

TIMING BELOW 100ps WITH SPARK COUNTERS: WORK PRINCIPLE AND APPLICATIONS

Yu.N. Pestov

(Invited talk given at the XXXVI Intern. Winter Meeting on Nucl. Phys., Bormio, 1998)

Gesellschaft für Schwerionenforschung mbH
Planckstraße 1 • D-64291 Darmstadt • Germany
Postfach 11 05 52 • D-64220 Darmstadt • Germany

TIMING BELOW 100ps WITH SPARK COUNTERS: WORK PRINCIPLE AND APPLICATIONS[†]

Yu.N. Pestov[§]

Gesellschaft fur Schwerionenforschung, Darmstadt

Abstract

The work principle of a spark counter with a localized discharge is described. A review of main counter characteristics as well as the key points of the latest R&D on the counter are presented. Possible large scale spark counter applications for the investigation of ion-ion collisions are discussed: ALICE - a dedicated heavy-ion experiment at the CERN Large Hadron Collider (LHC); the FOPI-Detector at the SIS accelerator of GSI, Darmstadt; NA49 - a fixed target experiment at the CERN-SPS.

[†] invited talk given at the XXXVI International Winter Meeting on Nuclear Physics, Bormio, 1998

[§] on leave from Budker Institute of Nuclear Physics, Novosibirsk

I. Introduction

The use of the spark counter offers a possibility of high time (up to 25ps) and position resolution (≈300μm) [1]. The detection efficiency is close to 100%, and the counting rate capability is by far sufficient for typical heavy-ion experiments. An, - in principal -, relative simple construction and a high intrinsic gain makes this type of counter a promising candidate for large scale applications, where high resolution at a low per-channel price is required. The idea of a spark counter with a localized discharge was proposed and realized at INP, Novosibirsk in 1971 [2]. The first application of these counters in a physics experiment was the pion formfactor measurement near the threshold at the electron-positron VEPP-2 collider, Novosibirsk in 1978-1985 [3]. In this work the spark counters were used both for particle identification by TOF and for the determination of geometrical characteristics of events. In the 1986-1991 the R&D work for e+e- colliders was continued in the frame of the SLAC-Novosibirsk collaboration. The activity for heavy ion applications developed in the period 1991-1998 in the frame of the ALICE* TOF collaboration including GSI Darmstadt, BINP Novosibirsk, JINR Dubna, MEPHI Moscow, RMKI Budapest, University of Marburg and NBI Copenhagen.

II. Work principle of the Pestov spark counter

II.1. TOF measurements with gas-filled parallel-plate detectors

A big advantage of gas-filled parallel-plate detectors (PPD's) for timing measurements is the homogeneous electric field in the gas gap. In this case every primary ionization gives immediate input to the timing signal independently on its position in the gas gap. The initial ionization appears in a PPD during the crossing of the gas gap by an ionizing particle. Hence, the crossing time puts a lower limit on the best possible time resolution value of

---

* ALICE - A Large Ion Collider Experiment- a dedicated heavy-ion experiment at the CERN LHC

PPD's, which is equal to about 10ps for relativistic particles for a gap size of a few mm.

The time resolution of TOF based on PPD's is defined both by the detector characteristics and the electronics. The ionization chamber has an ideal characteristics for timing measurements: a current output signal appears immediately and has a very good rise time. With an ideal electronics the time resolution of the ionization chamber could be on the level of ten picosecond. Unfortunately, present electronics is too noisy to detect small fast output pulses from ionization chambers.

The proportional PPD's have usually an avalanche gas amplification on the level of 10^4 [4]. The intrinsic time resolution of the detector improves with increasing gas gain. A time resolution of 250ps for relativistic particles with the gas mixture at atmospheric pressure was obtained at a higher gas gain. However, exposing this detector to low energy alpha particles yields spark probabilities in the order of 1 [5]. Because sparks could have an influence on the electrode deterioration, this effect produces additional limitation of the time resolution of proportional PPD's depending on the experiment conditions.

Spark counters with a gap size of 0.1mm have a time resolution value of up to 25ps, which was obtained at 12bar gas pressure [1]. Due to the very high gas amplification ($>10^9$) and the very good rise time of the output pulses the electronics problem for spark counter pulses is reduced dramatically. Concerning the input of fluctuations of the gas amplification on the TOF time resolution the high value of the electric field of 600kV/cm in the gas gap reduces them also.

It is important for further understanding to remind the physical principle of a standard parallel plate spark counter. The spark counter works in a streamer discharge mode, which could be realized in the gas mixture with good photon absorption properties. The spark development starts from a free electron, which produces a Townsend avalanche in the high electric field. When the number of electrons at the head of the avalanche reaches $\approx 10^8$ (Meek's criterion), a new, very fast streamer mechanism of ionization propagation appears. The positive and negative streamers produce a conducting plasma channel between the electrodes. The discharge current through this channel increases and finally a spark appears. Important to be aware, that the delay time of the discharge

development from an electron to a spark is mainly determined by the first Townsend avalanche. The fluctuation of this delay time is the sum of the fluctuations of the avalanche development and the occurrence of the streamer.

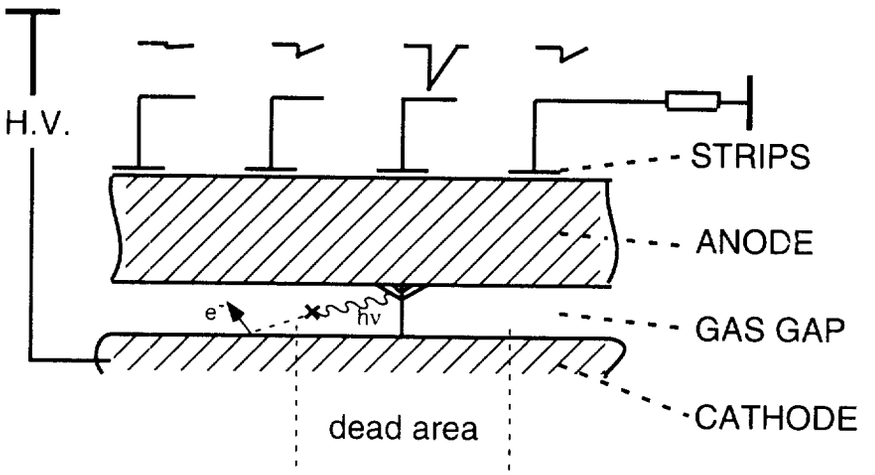

Fig. 1 Schematic layout of the Pestov spark counter counter.

II.2. Discharge localization

A standard spark counter has a rather small area of $\approx 1 cm^2$ because with increasing area the discharge energy in a spark becomes large enough to damage the counter electrodes. The counting rate of this counter is also limited by the dead time of more than 1ms, which is needed to remove ions from the gap (this value depends on the chosen gas mixture). To reduce these problems a new version of the spark counter was proposed [2]. The main modification consisted of the introductions of:

1) Resistive plate electrode (semiconducting glass)
2) Special gas mixture for photon absorption.

With this modification the performance spark counters changes dramatically. Now only a local area of electrodes is discharged by a spark. Because the high voltage drops only locally around each discharge the remaining counter area is still sensitive to particles. The overall rate capability of the spark counter improves drastically. The problem with the high energy in a spark also disappears due to the small local area of each discharge. There are few versions of practical realization of this idea in the spark counter design. At this paper we

consider the Pestov spark counter design which optimized for the best timing resolution. Fig. 1 shows the principle layout of this type of the counter.

A constant high voltage up two times higher than the threshold value for particle detection is applied to the counter electrodes. The counter is read out via strip lines positioned on the outer side of the resistive plate electrode. The wave impedance of each strip line is equal to 50Ω. Signals from sparks are detected by fast discriminators at both sides of each strip. The characteristics of each counter element, which is needed to realize a good counter performance are presented below:

1) A small gap size of 100μm was chosen because the time resolution value is proportional to the gap size.
2) The gas pressure of 12 bar is high enough to provide about 96% counter efficiency.
3) The bulk resistivity value of the anode must be more then 10^9 Ωcm to provide enough time to remove ions from the gap. The thickness of anode (2mm in this case) influences the size of the dead area and must be much thicker than the gap size.
4) The gas mixture should provide photon absorption from the low energy corresponding to the cathode work function to exclude secondary sparks by photon feed back.

Fig. 2 shows the absorption spectrum of the standard gas mixture consisting of 0.07 (bar) C_4H_6 + 0.3 C_2H_4 + 2.4 C_4H_{10} + 9 Ar = 12 bar.

The pressure of each component of this gas mixture was optimized. The Isobutane (C_4H_{10}) pressure of 2.4 bar was chosen to get better time resolution although just for discharge localization much less isobutane pressure would have been enough. The quantity of Ethylene (C_2H_4) in this gas mixture was minimized to the value, which provides stable counter performance. The quantity of 1,3-Butadiene was chosen for the ALICE application 4 times less than the optimal one in order to improve the counter live time proportionally. The absorption efficiency of this gas mixture is, as for most stable gases, very low around the work function of typical, e.g. aluminium or copper, cathode materials. The "gap" between the work function of the cathode material and the region where the photo-absorption cross section is sufficiently high is closed during a process called conditioning: the counter is operated together with a γ-

source in order to produce a thin polymeric layer on the surface of the cathode which shifts the work function to higher energies. After recording of 10^5-10^6 sparks/cm^2 the counter characteristics stabilize in time.

A new R&D program is in progress now with a goal to exclude conditioning with a γ-source from counter technology by using a cathode material with a high work function. Measurements with spark counters using tungsten cathodes demonstrated good performance without conditioning [6] but the counter life-time with the standard gas mixture became worse due to the Malter effect. Therefore, both a new gas mixture with low polymerization as well as a cathode material with a high enough electron work function without the need of a polymeric layer is sought. A potential candidate is a mixture with DME which has low polymerization [7], in combination with an aluminum nitride cathode, which has a high work function equal to >8ev [8]. The localization properties of this spark counter was recently demonstrated [9]. This result is considered as the promising beginning of a new spark counter technology without conditioning.

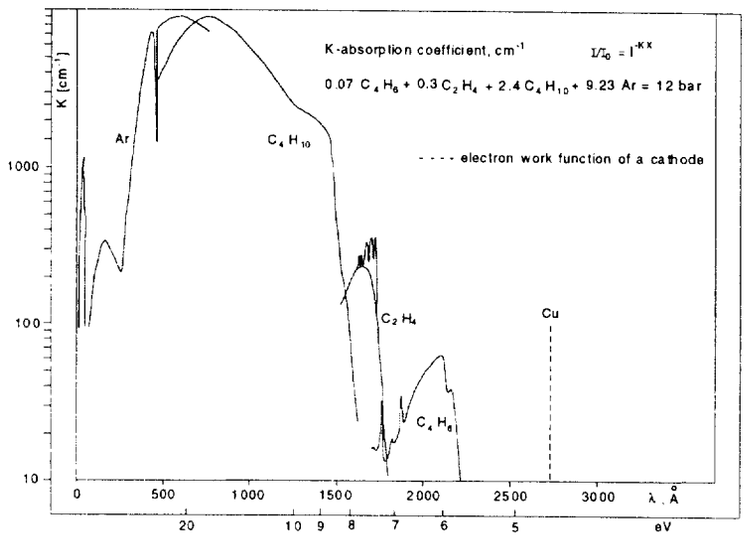

Fig. 2 Absorption spectra of the standard gas mixture.

II.3. Main counter and electronics characteristics

II.3.1. Working high voltage and output pulse parameters.

The counter threshold value for particle detection with the standard gas mixture (Fig. 2) is equal to about 3kV. The output pulse from each end of a fired strip has an average amplitude of 0.3V on a 50Ω load. The pulse rise time is less than 200ps but the trailing part of the signal varies due to after-pulses in the range of few nanosecond.

II.3.2. Discriminator.

Since the pulse rise time is very good, a fast leading-edge discriminator is essential to have a low walk within the amplitude variation. However, the intrinsic response time of standard leading-edge discriminators limits the time resolution to ≈70ps for the amplitude range of the spark counter. A novel type of the double threshold discriminator (DTD) provides essential compensation of the intrinsic response time. The idea of the DTD is based on two simultaneous time measurements for each pulse by two identical leading-edge discriminators with different thresholds [10]. The DTD provides 'on-line' a linear extrapolation of these two measurements to '0' threshold. The experimental value of the DTD walk turns out to be ≈10ps [10]. The chip version of the DTD is under development [11].

II.3.3. Efficiency

Fig.3 shows the measurements of the counter efficiency obtained at different high voltages. The solid curve on the Fig.3 corresponds to calculations based on the streamer theory [12].

II.3.4. Long term stability test

In total 8 counters have been operated satisfactorily over a period of more than 6 months. The integrated dose rate was equivalent to about 5 years LHC Pb running in the ALICE environment [11].

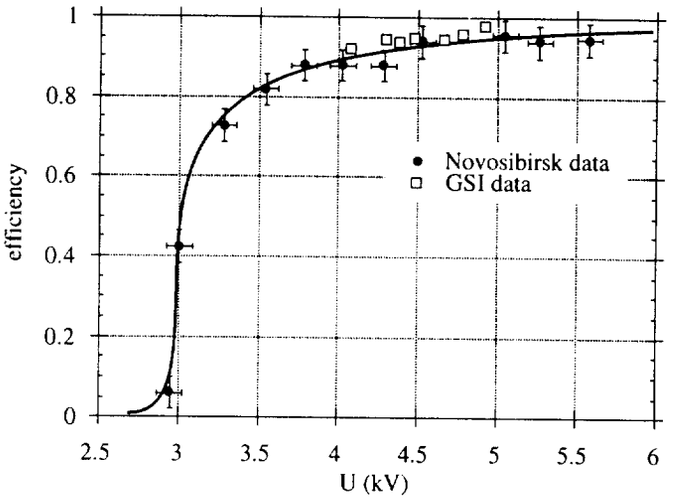

Fig. 3 Efficiency of the Pestov spark counter

II.3.5. Space resolution

A gap size of 0.1mm determines the accuracy of the coordinate measurements of the counter in the direction perpendicular to the electrode plane. The counter read out via strip lines (Fig.1) provides a two-dimensional reconstruction of the spark location in the electrode plane [13]. The position transverse to the strip direction is based on the measurement the distribution of the charge on strips for each spark. Then the well known center of gravity method is applied to find the spark position. From experimental data the transverse coordinate resolution of the spark counter turns out to be ≈0.3mm [13]. The position of a spark in strip direction is measured by the difference of the signal arriving time to the opposite ends of the strip. The longitudinal position resolution is limited by the resolution of electronics, mainly by the binning of the time digitizer, and is for the binning of 50ps equal to 2.5mm [13].

II.3.6. Time resolution

Measurements based on the FWHM of experimental distributions showed that the time resolution up to 25ps is possible with the spark counters [1]. However, the experimental timing distributions, taken between two counters have 'tails' which extend beyond the gaussian curve corresponding to the FWHM of the experimental distribution. We can exclude walk effects, i.e. the response of the frontend electronics, as source for large timing shifts. Trivial tails, i.e. from the

production of δ-electrons or reactions in the counter material itself are partially removed by requesting, within the resolution, the same position in the counters. As a test whether the remaining tail is inherent to counters properties or is solely due to insufficient clean-up cuts we have investigated its dependence on the applied overvoltage.

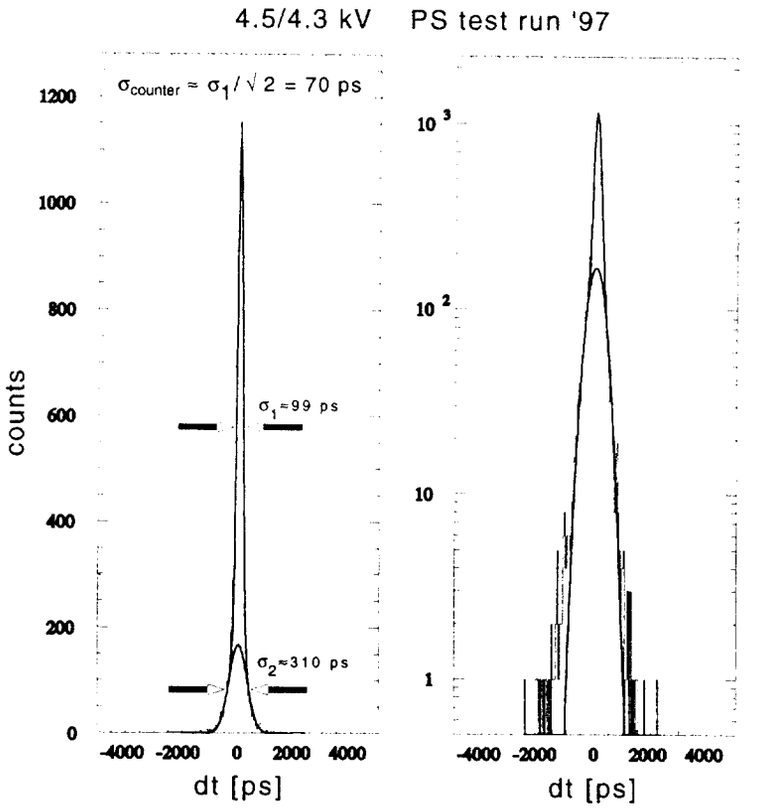

Fig. 4 Timing spectra between two counters. The voltages of the two counters were 4.5 and 4.3 kV, respectively. The right side spectrum is a representation in logarithmic scale.

In Fig. 4 and Fig. 5 we show the timing spectra between two counters. The voltage applied to the two counters was different, i.e. 4.5 and 4.3 kV in Fig.4 and 4.8 and 4.5 kV in Fig.5. In order to quantify the data two gaussian curves were fitted to the histograms. It should be noted that this is a purely mathematical concept, which may not correspond to a physical description of the origin of the tails. This is further outlined below. Firstly we notice that the time resolution of the central timing decreases with overvoltages as expected for the values applied. We also realise that the width of the tail improves with

overvoltage indicating that the origin of the tails is related to the discharge process itself. Quantitatively, the tails extend about 250ps (for 4.8/4.5 kV) and occur in less then 5% of all events.

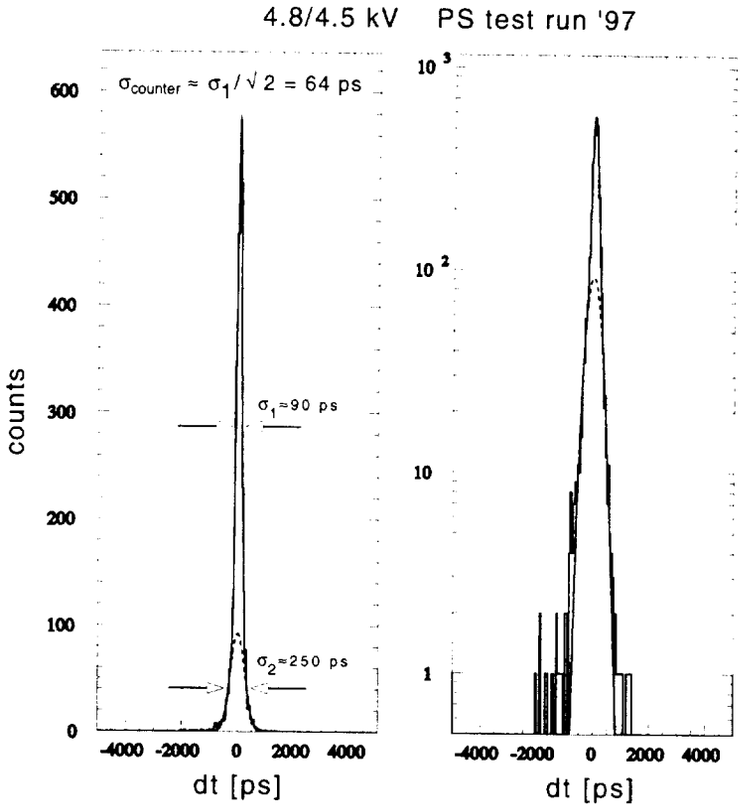

Fig. 5 Timing spectra between two counters. The voltages of the two counters were 4.8 and 4.5 kV, respectively. The right side spectrum is a representation in logarithmic scale.

Which processes in a gas counter, and in particular in a spark counter, could lead to tails?

1) One process, inherent to all gas filled counters, is the fluctuation of the avalanche development. A very stringent upper limit can be obtained from the following consideration: the maximum delay for the start of the avalanche is given by the electron drift velocity v_e and the gap size d by $\tau_{max}=d/v_e$, i.e., the time the electron needs to travel across the gap. For a drift velocity $v_e \approx 10^5$ m/s and a gap size $d=10^{-4}$m we get 1ns. To estimate the maximum deviation from the "right" timing we subtract the average delay time for the spark development which is, for 4.5kV, about 550ps.

Thus we obtain an upper limit for the shift due to avalanche fluctuation of $\tau < 500$ps.

2) A second process, inherent to spark counters only, could be the occurrence of an afterpulse without the full development of the avalanche to a streamer/spark. This may happen for those cases were the avalanche starts too close to the anode. Even though the avalanche does not multiply to 10^8 electrons, UV-photons are produced and may release secondary electrons from the cathode which themselves ignite a spark. An upper limit for the time delay by this process is given by $\tau = 20/(\alpha \cdot v_{electron}) \approx$ 550ns.

If we consider only these processes as sources for the tails the consequences are as follows:

1) the extent of the tails is limited by the underlying physics of the discharge process to times less than ≈0.5ns, smeared out with time resolution of ≈70ps. The scale parameter for this limit is the gap size; which, for the case of the spark counter is favourably small.
2) The probability for the second process depends on the absorption properties of the quencher gases. An optimized gas composition might reduce the occurrence of tail events.
3) The tails can be reduced by increasing the overvoltage as shown in Fig. 4 and Fig. 5.

More detailed investigations are needed to pin down and improve the tail problem.

III. Possible applications of the Pestov spark counters

Presently, we know three physics programs where a large scale spark counter array with good time resolution could be useful. For NA49 it is foreseen to install a Pestov TOF (PesTOF) counter array of an area of $1m^2$ inside the first vertex magnet to enhance particle identification in the backward rapidity hemisphere. The statistics for Pb+Pb collision at 158 AGeV is needed for rare processes requiring clean TOF identification, such as ϕ, $\Lambda(1520)$-production and KK, pp interferometry. The physics program of the FOPI collaboration, GSI includes the measurement of the K-flow and the ϕ-production yield for the

reaction Au+Au at the highest SIS energy (1.5 AGeV). FOPI proposes an upgrade in 1998/2000 with a barrel of Pestov counters to cover an area of 5.6m^2. For the investigation of hardron physics in Pb+Pb collisions at the center-of-mass energy of about 5.5 TeV/nucleon at ALICE, CERN detector a possible solution for particle identification is a TOF based on the Pestov counters with an area of up to ≈100m^2. The ALICE experiment is planed to be ready in 2006.

III.1. Particle Identification with PesTOF in FOPI

The FOPI collaboration at GSI evaluates various options to upgrade their TOF detector. One of the Pestov counters used in the long term stability test was installed in the FOPI experiment and operated together with the barrel detector during 4 weeks in a 1.5 GeV Au+Au run. The Pestov counter worked satisfactorily during the run. A plot of the mass separation obtained is shown in Fig. 6. Based on the experience gained during this run the FOPI collaboration proposes an upgrade of their TOF system with a barrel consisting of 155 Pestov counters. Each of the counters would be 90 cm long and read out with 16 strips. The radius of the barrel is 100 cm and it covers an area of 5.6m^2.

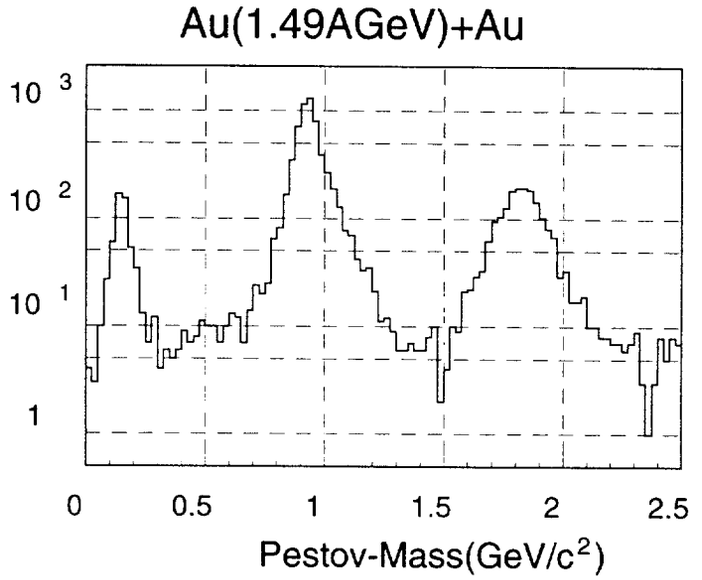

Fig. 6 Mass plot obtained with a Pestov counter together with the FOPI spectrometer for the reaction Au+Au at 1.5 GeV/A.

III.2. Particle Identification with PesTOF in NA49

The NA49 experiment at the CERN-SPS records charged particles over a large range of phase space with a set of 4 TPC's and additional time-of-flight walls. The two Vertex-TPC's are operated inside the Vertex-Magnets (MVTX(1/2)) with up to 1.5 T field strengths each. The particle identification is based on energy loss (dE/dx) measurements in the TPC tracking system and time-of-flight measurements in the forward rapidity hemisphere. NA49 studies p-p, p-Nucleus and Nucleus-Nucleus collisions at SPS-Energies. Fig.7 shows the experimental set-up. During the proton beam time of NA49 in fall 1997 an array of Pestov counters was operated at 4 m distance from the target behind VTPC-1 in the fringe field of the Vertex-Magnet-1 for the first time. The physical purpose of positioning of an additional Time-of-Flight array at this place is the extension of the particle identification to the backward rapidity hemisphere.

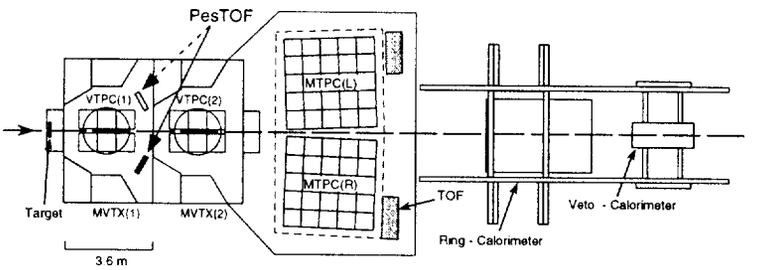

Fig. 7 Set-up of the NA49 experiment. The dashed arrow points to the foreseen installation of a second arm in fall '98.

The PesTOF array consists of 12 counters which were mounted on a common flange. The counters were staggered in two rows to provide full coverage in space with their active areas. Another purpose of this 'multiflange' is to distribute an equal fraction of the gas flow to all counters (see Fig.8). The total surface of the PesTOF array was 480x300mm^2. The manufacturing and test of a larger number of counters is an important step towards the production of more than 100 m2 of Pestov detectors for the CERN-LHC experiment ALICE. The machining of the counter anodes from a special semi-conductive glass and the production of the DTD, which is part of the front-end electronics, were done at BINP in Novosibirsk. For the readout of the charge signal from the 16 strips of

each counter a front-end QDC card produced by MEPHI, Moscow was used for the first time. All other counter parts were produced commercially. The operation of the counters during the 4 weeks of beam time at 4.5kV was very stable. For most of the counters the background counting rate was on the level of cosmic rays ($\approx 0.05 Hz/cm^2$) only.

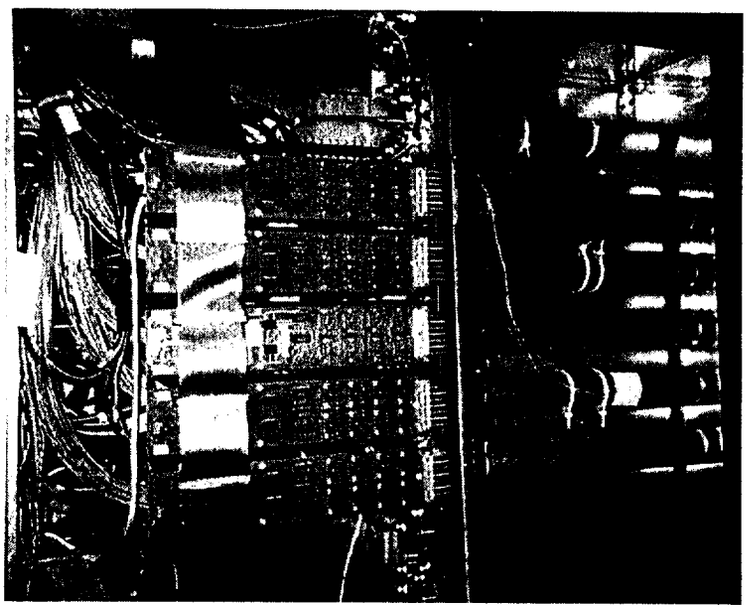

Fig. 8 Multiflange with 12 counters in the NA49 magnet.

The readout of the 384 channels of the PesTOF array was incorporated into the NA49 data acquisition. About 100k proton-nucleus events at 250 GeV/c have been recorded together with the full experiment. Only approximately 20% of these events have a track in the PesTOF array. A subsample of 50k p+Pb events was triggered by PesTOF. The average multiplicity in the PesTOF array for these p+Pb events was 1.2 particles per event. The PesTOF array is located on the side of VTPC-1 into which negatively charged particles are deflected by the magnetic field. The momenta of the particles are determined by the reconstruction of the trajectory in the TPC. The average laboratory momentum in the acceptance of the PesTOF array is 1.5 GeV/c. In Fig.9 the projections onto the horizontal and vertical axes are shown. The horizontal position distribution shows a slight increase of particle density on the side of the PesTOF array, which is closer to the beam axis. The population of particles in the vertical direction is symmetric with respect to the beam height, i.e., the bending plane.

The particle trajectories reconstructed in the VTPC1 where extrapolated to the PesTOF array through the magnetic field which decreases from 15 kGauss in the center of the TPC to approximately 1000 Gauss at the location of the PesTOF.

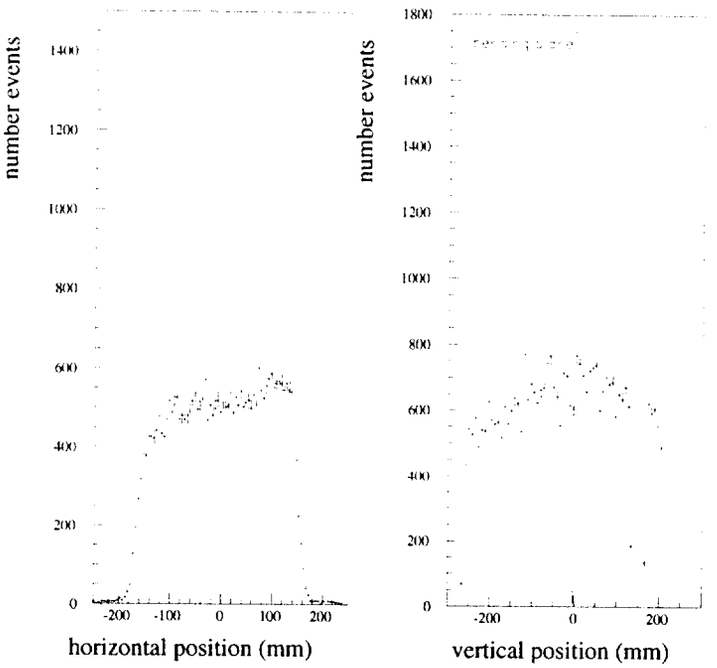

Fig. 9 Projections of the hit distribution in the PesTOF array onto the horizontal and vertical axes.

Fig.10 shows for 1000 events the difference between the hit position in the PesTOF and the prediction derived from the tracking of reconstructed tracks in the Vertex TPC-1. A preliminary evaluation of the matching accuracy gives 1.5mm in the vertical coordinate (transverse position in the counters) and ≈1cm in the horizontal coordinate (longitudinal position in the counters).

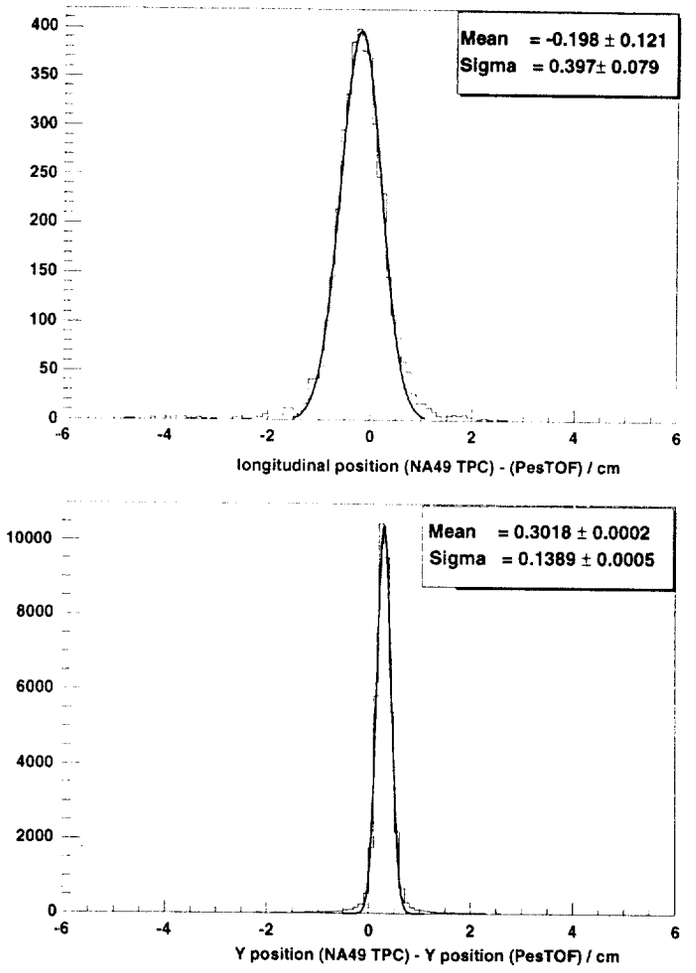

Fig. 10 Deviation of the predicted from the reconstructed hit position.

From the measured time-of-flight between start counter and PesTOF array, together with the reconstructed momentum and length of the trajectory from the target to the detector array, the mass of the particle can be calculated. In Fig.11 a preliminary result for the evaluated mass is shown. A cut on particles with momenta <1.5 GeV/c was applied. The mass distribution peaks at the pion mass. Only a small number of entries can be seen around the kaon mass, since the statistics is very low and the K/π ratio in the detector acceptance is only 3%. The width of the pion mass fit corresponds to a time resolution of about 125ps. The resolution is limited by the time resolution of the NA49 scintillator start counter of about 90ps. The Pestov counter array is planned to be enlarged in 1998 to up to 88 counters which will be located at both sides of Vertex TPC-1.

The total size of the array will then be $\approx 1m^2$. The position of the two PesTOF arrays was selected to extend the identification of kaons to the rapidity interval $1.2<y<2.2$. This improvement is essential for the determination of the complete rapidity distribution and thus the 4π-multiplicity of K^+ and K^- mesons. It will also enable the reconstruction of ϕ-mesons.

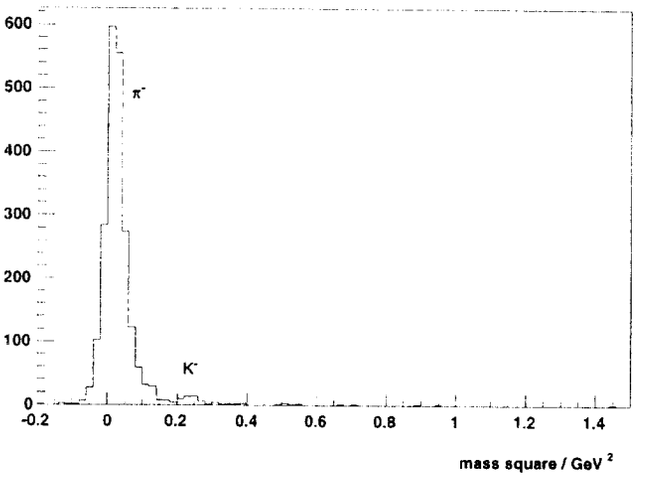

Fig. 11 Very preliminary mass plot.

IV. Conclusion

While most of the principal questions of the spark counter physics are solved, a few, mainly related to the optimization of the counter performance, remain. On the technological side, the main problems are related to the choice of the proper materials and procedures for mass production and assembly as well as to the development of fast, integrated electronics. The possible applications in physics experiments -NA49 CERN, FOPI GSI and ALICE CERN- open the perspective of further development of the counter technology from an counter array area of $1m^2$ (NA49) to $\approx 100m^2$ (ALICE).

V. Acknowledgement

This review paper includes the result of the work of many collaborators. It is a pleasure for me to thank my colleagues who have in different periods of time participated in the R&D work on the spark counters. I would like to acknowledge my collaborators at the GSI, where the main part of the R&D

work on the spark counters for the heavy-ion applications was done. I am grateful to the GSI for very good hospitality.

VI. References

[1] Yu.N.Pestov,Proc.4th San Miniato Topical Seminar,World Scientific,1991,156.

[2] V.V.Parchomchuck, Yu.N.Pestov and N.V.Petrovykh, NIM 93 (1971) 269

[3] I.V.Vasserman, P.M.Ivanov, Yu.N.Pestov et al. Jadernaja Fisica, 28 (1978) 968; Jadernaja Fisica, 33(1981)709.

[4] Glenn F.Knoll,Radiation detection and measurement,John Wiley & Sons, 1979, 210.

[5] A. Smirnitsky et al., PPC for ALICE – private communication

[6] Yu.N. Pestov, Nucl.Instr.Meth. A265 1988 150.

[7] L.Alunni et al., Nucl.Instr.Meth, A348 (1994) 344.

[8] J.Pastrnak and A.N.Trukhin, Czech.J.Phys.B27 (1997).

[9] U.Frankenfeld, H.Sann et al. GSI-Preprint-98, 1998, in print.

[10] A.R.Frolov, T.V.Oslopova, Yu.N.Pestov, Nucl.Instr.Meth.A356(1995)447-451.

[11] PesTOF collaboration, GSI-Preprint-98-14, Marz 1998.

[12] V.D.Laptev and Yu.N.Pestov, Pribori i Tekhnika Eksperimenta N6(1975)41-42.

[13] A.R.Frolov, Yu.N.Pestov and V.V.Primachek, Nucl.Instr.Meth. A307(1991)497- 503; E.Badura, J.Eschke, H.Gaiser at al.Nucl.Instr.Meth. A372(1996)352-358.